JCBI
Journal of Computing & Biomedical Informatics
ISSN: 2710 - 1606
Volume 05 Issue 02
2023

Research Article
https://doi.org/10.56979/502/2023

Multi-classification of Skin Cancer Using Multi-model Fusion Technique

Hamna Ayesha[1*], Ahmad Naeem[1], Ali Haider Khan[2], Kamran Abid[1], and Naeem Aslam[1]

[1]Deparment of Computer Science, NFC-IET, Multan, Pakistan.
[2]Department of Software Engineering, Lahore Garrison University, Lahore, Pakistan.
[*]Corresponding Author: Hamna Ayesha. Email: hamnaayesha66@gmail.com.

Received: April 15, 2023 **Accepted:** August 21, 2023 **Published:** September 17, 2023.

Abstract: Skin cancer is increasingly common worldwide, with melanoma and basal cell carcinomas being the primary subtypes, responsible for most of the related deaths. Therefore, screening for early identification and classification is essential for proper treatment, a task achievable through deep learning techniques. While numerous studies have addressed this problem domain, challenges such as limited accuracy, deployment on edge devices, computational costs, execution times, and manual feature extraction procedures persist. In this research work, a novel deep learning architecture is proposed to address these issues. Three pre-trained deep learning architectures are utilized namely VGG-16, VGG-19, and ResNet-50, through transfer learning to develop a composite model named "Multi-Model Fusion for Skin Cancer Detection (MMF-SCD)". A composite feature vector is generated by these CNN models and passed through a final dense layer with a SoftMax activation function for skin cancer classification. Adam optimization algorithm is applied. TensorFlow and Keras libraries are employed to develop MMF-SCD model. Rectified linear unit is applied as an activation function for the output of convolutional layers of MMF-SCD. This model is developed on Jupyter notebook using open-source web platform namely google Collaboratory in python programming language. The dataset, retrieved from public dataset repository, consists of seven of the most common skin cancer diseases: actinic keratosis, basal cell carcinoma, dermatofibroma, melanoma, nevus, pigmented benign keratosis, and vascular lesion. MMF-SCD has demonstrated significantly improved accuracy compared to previous studies, achieving an accuracy gain of 97.6%.

Keywords: Classification, Deep learning, transfer learning, skin cancer, VGG-16, VGG-19, ResNet-50, multi-model fusion.

1. Introduction

Skin cancer is a global health challenge characterized by the uncontrollable growth of abnormal skin cells, with melanoma being the deadliest form, emphasizing the critical importance of early detection and accurate diagnosis [1]. Traditional methods, including Dermoscopy and biopsies, have limitations, prompting the exploration of innovative solutions [2]. Although Artificial Intelligence (AI) has emerged as a promising tool in healthcare, many AI studies in skin cancer detection have grappled with the issue of false diagnoses [3]. Dermatologists face challenges in accurately distinguishing between malignant and benign lesions due to their visual similarities [4]. Dermoscopic images have been used in various studies for skin cancer classification [5]. Existing literature has explored various techniques, including machine learning

algorithms and deep learning models [6] like Convolutional Neural Networks (CNN), to enhance skin cancer classification accuracy [7]. However, these studies often encounter obstacles related to data scarcity and computational resources [8], [9]. Achieving a robust and generalized deep learning model with a limited dataset remains a challenge, considering the intricate visual resemblances between different types of skin cancers and the subtle variations within the same type. Transfer learning based on deep learning techniques have resulted efficient performance for skin cancer diagnosis [10]. Major skin cancer types are actinic keratosis (ACK), basal cell carcinoma (BCC), dermatofibroma, melanoma, nevus, pigmented benign keratosis, and vascular lesion. ACK is a keratosis lesion that develops on adult skin repeatedly exposed to light. It appears as a dry, rough, and sometimes pigmented lesion of varying thickness and size [11]. BCC often originates in the deepest layer of the skin's epidermis, where basal cells are located [12]. Dermatofibroma belong to the group of cancers caused by the accumulation of various cell types in the skin's dermis layer. They are typically 2-3 mm (about 0.12 in) in size, have a purplish-brown color, possess a firm structure, and feel uncomfortable to the touch [13]. Melanoma skin cancer is serious. It starts in the skin and can spread to other parts of the body. They might also itch, bleed, and get bigger compared to regular moles [13]. Melanocytes are special cells in the skin that make pigment. Sometimes, they can form a lump called nevus pigmentosus, which can look like a birthmark or mole [13]. Pigmented benign keratosis represents common and harmless skin growth. These growths encompass lichenoid keratosis, seborrheic keratosis, and solar lentigo found on the back, chest, head, and neck, and they have a light skin-colored brown or black appearance [14]. Vascular lesion refers to an abnormal gathering or formation of blood vessels on or within the skin. These lesions can exhibit various appearances, such as hemangiomas, port-wine stains, and birthmarks resulting in visible pink, red, or purple discolorations on the skin's surface [15].

This study aims to consolidate the existing knowledge in the development of an automatic skin cancer classification system, delving deep into recent advancements and challenges faced by researchers [16]. The proposed research investigates the feasibility of building a high-accuracy deep learning model despite the constraints posed by a limited dataset [8], [9]. To achieve this, the study merges features extracted from multiple CNN-based architectures; implements transfer learning techniques, and optimize various model parameters [7]. In this context, the significance of this work lies in its potential to significantly impact the field of dermatology [7]. A successful automated system would alleviate the burden on healthcare professionals, enabling more individuals to undergo routine screenings efficiently [4]. The contribution of this research lies in its innovative approach to merging deep learning models, addressing the challenges of limited data, and striving for improved accuracy in skin cancer classification [16].

The dataset for this study comprises dermoscopic images, and the methodology involves implementing a composite model using a deep learning architecture [16]. This novel approach aims to minimize false predictions and enhance the efficiency of feature extraction algorithms [7]. The significance of this work offers a practical solution to a critical healthcare challenge [16].

The organization of this paper encompasses a detailed exploration of existing literature, highlighting the limitations of previous studies [4]. The subsequent sections delve into the methodological analysis, experimental results, and findings, providing a comprehensive overview of the research process and outcomes [4]. This structured approach ensures a thorough examination of the problem and the proposed solution, contributing valuable insights to the field of skin cancer detection and classification [16] [7].

2. Literature Review

The rapid advancements in deep learning and convolutional neural networks (CNNs) have sparked significant progress in the automated detection and classification of skin cancer. These developments are

crucial for early diagnosis and effective treatment. Researchers have explored diverse datasets, such as HAM10000 and ISIC 2020, aiming to classify a wide range of skin lesions including melanoma, basal cell carcinoma, squamous cell carcinoma, and nevi. Utilizing innovative methodologies and deep learning techniques, these studies have demonstrated the potential to transform dermatological diagnosis, offering substantial support to healthcare professionals.

The study by Sevli et al. [15] centered on the use of a Convolutional Neural Network (CNN) to classify several types of skin lesions with remarkable accuracy, achieving 91.51%. Compared to prior research, this CNN model demonstrated superior performance. Dermatologists evaluated the model, confirming its ability to diagnose skin lesions with 90.28% accuracy in practical scenarios. Furthermore, in the second phase, the model corrected dermatologists' misdiagnoses by 11.14%, emphasizing its potential to enhance the precision and efficiency of skin cancer diagnosis. The study by Gouda et al. [16] main goal is to use intelligent systems for categorizing skin diseases, considering the challenges posed by skin texture and the visual resemblance between different conditions. They worked with a dataset of 25,331 clinical-skin disease images spanning eight categories, using advanced techniques like Residual Neural Network (ResNet). The result was an impressive 92% accuracy in diagnosing different skin lesions, offering valuable support to dermatologists for early and precise disease identification and treatment planning. Javaid and colleagues [17] presented a novel method that combines image processing and machine learning to classify and segment skin lesions into non-cancerous or cancerous categories. It employs feature extraction techniques such as HOG and GLCM, OTSU thresholding, and contrast stretching. Dimensionality reduction via PCA and class imbalance handling with SMOTE are used. The authors introduce a unique wrapper-based feature selection method and evaluate various classification algorithms, with Random Forest (RF) achieving the highest accuracy of 93.89% on the ISIC-ISBI 2016 dataset, presenting the effectiveness of their approach in enhancing skin lesion classification and segmentation.

This study [18] evaluated the performance of a convolutional neural network (CNN) in classifying clinical images of pigmented skin lesions, comparing it with dermatologists. They collected a dataset of 5846 images from 3551 patients and trained an FRCNN model, achieving 86.2% accuracy in six-class classification and 91.5% accuracy in distinguishing benign from malignant lesions. The FRCNN model outperformed dermatologists and holds the potential for improving skin cancer prognosis when implemented in clinical practice. This study [19] aimed to enhance skin cancer recognition using deep learning and develop a mobile application. They reviewed medical knowledge on skin cancer and recent research, then tested 11 CNN architectures on the HAM10000 dataset with seven skin lesion classes, achieving the best results with DenseNet169, which had an accuracy of 92.25%, recall of 93.59%, and F1-score of 93.27%. They also created an Android app for two-class skin lesion classification (benign or malignant) and provided sun exposure recommendations based on UV radiation, skin type, and sunscreen use, marking a significant advancement in skin cancer diagnosis and user awareness.

Convolutional neural network (CNN) is a sub-field of deep learning; it has gained success in various domains of life including medical image diagnosis. It is being applied in computer vision-based tasks and has effective results in image recognition and segmentation [20]. CNN is an efficient tool that automatically extracts relevant features (edges, shapes, color, texture) by employing its hidden layers (convolutional & pooling), it has also ability to extract complex patterns and features from image, audio, and video data due to implementation of ReLU (Rectified linear unit) non-linearity. The architecture of CNN consists of various convolutional and pooling layers. The major layers of this network are convolutional and pooling followed by dense layers.

Due to the automatic feature extraction, classification, and identification characteristics, CNN has gained remarkable achievement in the deep learning domain for applied studies in medical image analysis. An automated CNN-based skin lesion classification approach was proposed in the study [21]. The author applied three pre-trained CNN algorithms named: ResNet18, vgg16, and ALexNet using a transfer learning approach for deep feature extraction. These features were then used to train the model and classify them using a machine learning classifier support vector machine (SVM) on the ISIC 2017 skin cancer image dataset which resulted in an average accuracy rate of 90%.

A technique for classifying 12 skin lesions was proposed by Mendes et al. [22] using the CNN-based architecture ResNet-152 algorithm. The dataset consists of 3,797 digital images of skin lesions. This proposed technique resulted in 90% and 96% AUC for basal cell lesions and melanoma, respectively. The data augmentation technique was applied to the dataset and testing was conducted for the evaluation of the model. This study [63] aimed to develop a rapid skin cancer classification system using deep CNN and an ECOC SVM. They collected RGB images of skin cancers from the internet and pre-processed them to remove noise. By employing a pre-trained AlexNet for feature extraction and an ECOC SVM for classification, the system achieved high accuracy, with the best results for squamous cell carcinoma (95.1%) and actinic keratosis (98.9%), while the lowest values were observed for basal cell carcinoma (91.8%), squamous cell carcinoma (96.9%), and melanoma (90.74%).

The study [23] focuses on improving dermatological diagnosis accuracy and presents a MATLAB-based system for identifying and classifying skin lesions as normal or benign. They utilized the K-nearest neighbor (KNN) approach for its efficiency and achieved an outstanding classification accuracy of 98%, addressing the need for quick and reliable diagnoses in dermatology. The primary aim of this research work by Murugan et al. [24] is the segmentation and classification of skin lesions. The methodology employed watershed segmentation to partition these lesions, extracting various features such as shape, the ABCD rule, and GLCM (Gray Level Co-occurrence Matrix) from these segmented areas. Subsequently, the study utilized three distinct classifiers: kNN (k Nearest Neighbor), Random Forest, and SVM (Support Vector Machine) for lesion classification. Notably, among these classifiers, the SVM classifier demonstrated superior performance in accurately classifying skin lesions with an accuracy rate of (89%) while KNN (69%) and RF (76%) had low performance.

The research by Nie et al. [24] introduces the You Only Look Once (Yolo) algorithms, utilizing Deep CNNs to detect melanoma. V1, V2, and V3 are the variants of the Yolo algorithms, which resize input images and split them into cells. By considering the object's position within a cell, the network predicts both the object's bounding box and class confidence score. The study achieves a mean average precision (mAP) of over 0.82 with only a 200-image training set, highlighting its effectiveness in lightweight systems for melanoma detection. In another study, Nie et al. [9] provokes the problem of insufficient data for effectively classifying melanoma using Deep Convolutional Neural Networks (DCNNs) within Swedish hospital surroundings. To address this issue, the paper recommends implementing K-Fold cross-validation in combination with a DCNN algorithm and utilizing Vgg16 for feature extraction. The outcomes demonstrate a significant enhancement in predictive accuracy when dealing with small skin cancer datasets. Through experiments utilizing 760 training images and a 5-Fold cross-validation approach, the study produced five models that achieved an accuracy rate of 63.35% when applied to new images.

The study by Atta et al. [25], proposed a robust methodology for the classification of skin cancer. The dataset consists of 3600 images, each sized at 224 x 224 pixels, and is divided into two classes: Malignant and benign, with each class containing 1800 images. To establish a reliable classification system, a

Convolutional Neural Network augmented with fully connected layers was utilized. Remarkably, the model achieved a significant accuracy of 86.23% while keeping computational efficiency integral.

In the study by Akter et al. [26], various deep-learning models are utilized to categorize skin lesions, specifically for distinctive skin cancer from other types of skin abnormalities. The study involves preprocessing and augmenting data from the HAM10000 dataset, which encompasses seven diverse classes of skin lesions. These models encompass Convolutional Neural Networks (CNN) as well as transfer learning models namely Xception, Densenet, Mobilenet, Resnet-50, VGG-16, and Inceptionv3, achieving accuracy rates ranging from 77% to 90% in detecting skin cancer. Besides, the study explores the use of stacking models, but it observes that their performance is comparatively lower, with the highest accuracy among them reaching 78%.

Tahir et al. [27] introduced a novel deep learning-based skin cancer classification network called DSCC_Net and assessed its performance on three standard datasets (ISIC 2020, DermIS, and HAM10000). DSCC_Net achieves remarkable results, including a 94.17% accuracy, 99.43% AUC, 94.28% precision, 93.93% F1-score, and a 93.76% recall when classifying four types of skin cancer (basal cell carcinoma, melanoma, squamous cell carcinoma, and Nevus). Comparative analysis against six established deep networks highlights DSCC_Net's superiority, highlighting its potential to assist dermatologists and healthcare professionals in accurately diagnosing skin cancer.

The primary objective of the research by Mridha et al. [28] was to develop strong deep-learning models capable of effectively classifying skin cancer while tackling class imbalance issues and offering transparency in decision-making. The study also introduced a comprehensive healthcare system accessible via an Android app. Utilizing the HAM10000 dataset; the researchers fine-tuned a CNN model with various functions. Furthermore, they devised an Explainable Artificial Intelligence (XAI) system employing Grad-CAM and Grad-CAM++ to explain the model's decision process. This innovative system achieved an 82% accuracy in classifying skin cancer, with a minimal 0.47% loss accuracy, thereby aiding physicians in early-stage skin cancer diagnosis.

The effectiveness of ResNet50, Support Vector Machines (SVM), and MobileNet is assessed by Mampitiya et al. [29] for classifying the HAM10000 skin cancer dataset, encompassing seven cancer types. SVM incorporates the Synthetic Minority Oversampling (SMO) method and Histogram of Oriented Gradient (HOG) features with Principal Component Analysis (PCA) for dataset balancing. Furthermore, six traditional machine learning approaches are compared, using F1 Score, accuracy, precision, and recall as evaluation matrices. The findings highlight SVM's outstanding performance, achieving an impressive accuracy rate of 99.15%.

In the research by Polat et al. [30], two approaches are introduced for the automated classification of skin diseases: a self-contained Convolutional Neural Network (CNN) model and a strategy combining CNN with one-versus-all classification. No preprocessing methods were utilized; instead, the raw dermatology images were directly utilized in training and testing the CNN. The standalone CNN achieved a 77% accuracy in classifying seven skin disease categories, while the combined CNN and one-versus-all approach demonstrated outstanding performance with an impressive accuracy of 92.90%. HM10000 skin cancer public dataset with seven categories named: Vascular lesions, Actinic keratosis, Basal cell carcinoma, Dermatofibroma, Melanoma, Benign keratosis, and Melanocytic type was utilized for training of models.

In this investigation by Ratul et al. [31], dilated convolution in deep learning is examined for its ability to enhance accuracy without adding computational complexity, in contrast to conventional CNN methods. The study applied transfer learning to four widely used architectures (MobileNet, VGG-16, VGG-19, and InceptionV3) using the HAM10000 dataset, which comprises 10,015 dermoscopic images across seven skin

lesion categories, presenting class imbalances. The achieved top-1 accuracy on dilated versions of these architectures ranged from 85.02% to 89.81%. Particularly, Dilated InceptionV3 exhibited the highest classification accuracy, recall, precision, and f-1 score, outperforming other approaches for skin lesion classification on this complicated dataset characterized by class imbalances.

The research by Rashid et al. [32] presents an innovative deep transfer learning approach employing MobileNetV2 for melanoma classification, differentiating between malignant and benign skin lesions. The model's effectiveness is evaluated on the ISIC 2020 dataset, which exhibits a significant class imbalance, with less than 2% malignancies. To moderate this imbalance and improve dataset variety, various data augmentation methods were employed. The proposed method, applied to the ISIC-2020 challenge dataset, attains an impressive diagnostic accuracy of 98.2%, highlighting its effectiveness in skin cancer classification.

In the tapestry of scientific discovery, Ali et al. [33] have woven a masterpiece: a Deep Convolutional Neural Network (DCNN) model. Like a skilled artist, it delicately refines, reducing noise, harmonizing colors, and chiseling features. With a sprinkle of magic, it multiplies its data, enhancing its vision. This enchanted dance boosts accuracy, painting the world of skin lesion classification in vibrant hues. The performance of the DCNN model is evaluated against several transfer learning models, including AlexNet, ResNet, VGG-16, DenseNet, and MobileNet, using the HAM10000 dataset. The results demonstrate the proposed model's excellence, achieving impressive training and testing accuracy rates of 93.16% and 91.93%, respectively. A fine-tuning method is applied to the pre-trained Xception model by Moataz et al. [34] for classifying skin lesions. Additional layers are incorporated into the Xception model, and all model weights are retrained. This fine-tuning process is carried out using the HAM10000 dataset with seven classes, and data imbalance is mitigated through augmentation. Comparative assessments showcase the effectiveness and dependability of the proposed model, which achieves an impressive 96% accuracy in discerning various skin cancer classes when working with a balanced dataset.

An innovative automated method is introduced by Saba et al. [35] for detecting and recognizing skin lesions, employing a deep convolutional neural network (DCNN). The approach consists of three key stages: enhancing contrast using HSV color transformation and fast local Laplacian filtering (FlLpF), extracting lesion boundaries through a color CNN with XOR operation, and performing comprehensive feature extraction via transfer learning with the Inception V3 model. Feature fusion is achieved using the hamming distance (HD) approach, and an entropy-controlled feature selection method is introduced for selecting relevant features. The method's performance is assessed on the PH2, ISBI 2016, and ISBI 2017 datasets having benign and malignant dermoscopic images, resulting in impressive accuracies of 98.4%, 95.1%, and 94.8%, respectively, surpassing existing methods. The summary of current literature is presented in Table 1.

Table 1. Related Work Analysis

Article/Ref	Dataset	Contribution/Method	Results/Finding	Weakness/Limitations
[22]	1470 images	Data augmentation, CNN based ResNet-152 algorithm	AUC (BC: 91%, melanoma: 96%)	Limited representation of benign lesions, lack of diversity
[36]	3,753 dermoscopic images	CNN feature extractor and SVM classifier	Accuracies: BSS (94%), SCC (95%), AK (98%)	Class imbalance, limited scalability

[23]	100 images	KNN, MATLAB classification	98% accuracy	Small dataset, restricted lesion categories
[24]	Not specified	Watershed segmentation, GLCM, ABCD rule, SVM, KNN, RF classifiers	89% accuracy from SVM	Limited scalability, class imbalance
[8]	200 images	Yolo V1, V2, V3, deep CNN	mAP: 0.82	Small training set, potential over fitting
[9]	1000 images	Deep CNN, K-fold cross-validation, Vgg16 for feature extraction	63% accuracy at 100 epochs	Limited accuracy on new data, class imbalance
[25]	3600 images	CNN for feature extraction and fully connected layers	86.23% accuracy	Computational efficiency not specified
[26]	10,015 dermatoscopy images	Xception, Densenet, Mobilenet, Resnet-50, VGG-16, Inceptionv3, CNN	90% maximum accuracy	Limited interpretability of deep models
[27]	ISIC 2020, DermIS, HAM10000	DSCC_Net, deep learning	94.17% accuracy	Lack of explanation of model decisions
[28]	HAM10000 dataset	Deep learning, Android app, fine-tuning of CNN, Explainable AI	82% accuracy	Limited validation in real-world clinical settings
[29]	HAM10000	ResNet50, SVM, MobileNet	99.15% accuracy	Class imbalance not addressed
[30]	HM10000	Automated classification, CNN	Accuracy: 92.90%	Lack of detailed methodology description
[31]	HAM10000	MobileNet, VGG-16, VGG-19, InceptionV3	89.81% accuracy rate	Limited discussion on computational efficiency
[32]	ISIC 2020 dataset	MobileNetV2	Accuracy: 98.2%	Class imbalance and dataset variety issues
[33]	HAM10000	Deep CNN, AlexNet, ResNet, VGG-16, DenseNet, MobileNet	Training: 93.16%, Testing: 91.93% accuracy	Limited transparency in model decisions
[34]	HAM10000	Xception model, augmentation of images	96% accuracy	Small dataset, potential over fitting
[35]	PH2, ISBI 2016, ISBI 2017 datasets	CNN, Inception V3	Accuracy ranges: 94-98%	Limited discussion on generalizability to diverse datasets

3. Proposed Methodology

The workflow architecture of proposed study is presented in Figure 1 for skin cancer classification. A public dataset ISIC is employed for experiment of this study. This dataset is split into two portions. Train

set is 80% of dataset, whereas remaining is 20% of dataset is for validation set. This image data consists of dermoscopic skin lesions that undergo pre-processing steps named: resizing and rescaling. Data augmentation is conducted using ImageDataGenerator function based on keras for training proposed CNN model. Three CNN algorithms: VGG-16, VGG-19, and ResNet-50 are applied for feature extraction by means of transfer learning approach. Then these features (feature set of each algorithm) are combined to generate a final feature matrix. Nadam is utilized as optimization algorithm for training of model. A composite model "Multi-Model Fusion for Skin Cancer Detection (MMF-SCD)" is developed using features of these three algorithms and then trained on intended dataset. Classification is performed using fully connected layers with SoftMax activation function.

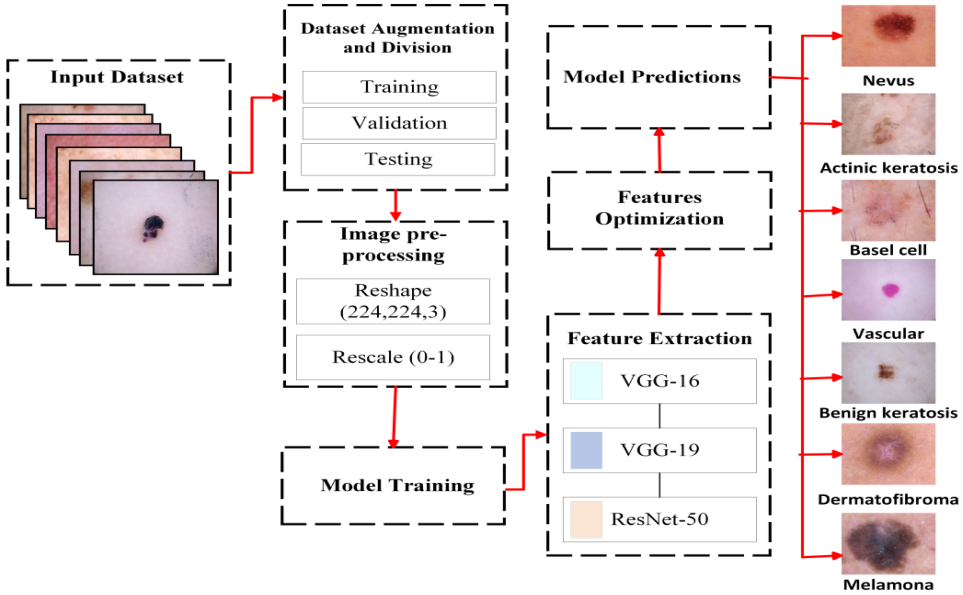

Figure 1. Proposed methodology block diagram showing major steps of this study namely: input dataset, data augmentation and division, image pre-processing, feature extraction and optimization, and model predictions.

The proposed methodology consists of various steps as shown in Figure 1. These steps of this proposed methodology are explained in the next sections. Skin cancer ISIC dataset is accessed and data augmentation technique is applied on them. Then whole dataset is divided into training, validation and testing sets. Image pre-processing techniques are applied that includes reshape/resizing and rescaling. A composite model "MMF-SCD" is designed and three deep learning based CNN models named: VGG-16, VGG-19, and ResNet-50 are utilized for feature extraction during model training process. These features are then optimized and classification of skin cancer diseases is conducted using fully connected/dense layers by utilizing SoftMax activation function, so model can make predictions.

3.1 Dataset augmentation and division

The ISIC dataset for skin cancer classification employed in this study is publically accessible and available at Kaggle website named: Skin Cancer [37]. It consists of seven skin cancer lesions named: actinic keratosis, basal cell carcinoma, dermatofibroma, melanoma, nevus, pigmented benign keratosis, and vascular lesion. In the next phase, data augmentation is applied by utilizing an image data generator technique from TensorFlow to increase the number of dermoscopic skin cancer images. This approach augments both the training and validation datasets in real-time during the MMF-SCD model's training phase, eliminating the need for pre-processing. Through the augmentation phase, this method generates a diverse set of images with the objective of preventing from overfitting and enhancing the model's ability

to accurately classify skin cancer diseases. The parameters name and their values set during data augmentation are presented in Table 2.

Table 2. Data augmentation parameters and their description

No.	Name	Value	Description
1	Rotation range	20	The degree of random rotation for each image is set to 20.
2	Fill mode	Nearest	This mode is set to nearest to fill the spaces created during rotation of images.
3	Width shift range	0.2	Value is set to 0.2 to control the range of horizontal shift of images.
4	Vertical flip	True	All the images are flipped in vertical manner.
5	Horizontal flip	True	All the images are flipped in horizontal manner
6	High shift range	0.2	Value is set to 0.2 to control the range of hight shift of images.

The details of these images are presented in Table 3. Total number of images in training and validation are 8,512 and 1,503 respectively as shown in Figure 2 as bargraph.

Table 3. Class distribution of Images

Disease Name	Distributions for training	Distributions for validation
Actinic keratosis	278	49
Basal cell carcinoma	437	77
Dermatofibroma	98	17
Melanoma	946	67
Nevus	5,699	100,6
Pigmented benign keratosis	934	165
Vascular lesion	120	22

The objective of this division is to enhance and assess the model's performance. The training dataset is employed to train the proposed MMF-SCD model with its biases and weights being adapted during the learning phase to reduce misclassifications. On the contrary, the validation dataset is distinct and used to

optimize the MMF-SCD's hyperparameter settings, such as the learning rate. Its primary purpose is to prevent overfitting and evaluate the model's ability to generalize during the training process.

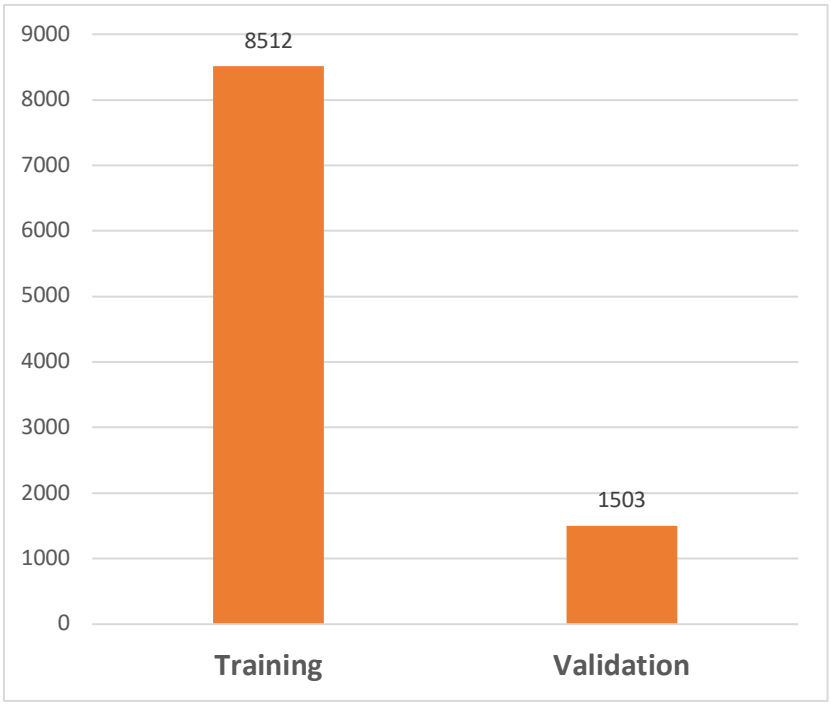

Figure 2. Dataset division

The dataset images are divided into two main portions. A large number of images (8512) are allocated for training and (1503) images are kept for validation. A small number of images (141 in count) are kept separate for testing purpose after model development (training and validation) process.

3.2 Data pre-processing

Image preprocessing plays a vital role in enhancing image quality and streamlining dataset manipulation by eliminating noise and anomalies. Within this study, the dataset comprised more than 10,000 dermoscopic skin cancer images, each with varying resolutions. Given that all images surpassed the resolution of 224 × 224, it became necessary to pinpoint the region of interest (skin lesion) and eliminate any extraneous elements from each image as shown in figure 3. All images of dataset are pre-processed by advanced two methods: resizing and rescaling to make them uniform and reduce computational complexity by employing TensorFlow and Keras based procedures.

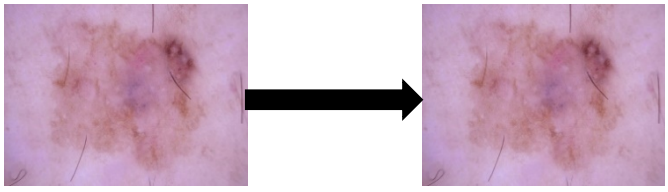

600x450 224x224

Figure 3. Resizing process of images, the actual dimensions of images are 600x450 whereas resized dimensions are 224x224 to meet the model requirement

The original size is 600x450 in dimensions which is resized by down-sampling method to 224x224 as shown in Figure 3. By resizing process, all the images have same dimensions which help MMF-SCD to efficiently perform and result in improved high generalization ability.

The next step is rescaling, in this every pixel of image is rescaled from original range of 255 to 0-1 by dividing them to 255. Presume *img* is the input image, the rescaled image is acquired as follows:

$$rescaled\_image = \frac{img}{255} \quad (1)$$

3.3 Feature extraction

Three models are applied for features extraction [38] namely: VGG-16, VGG-19, and ResNet-50. These models are explained in the following along with their fundamental layers.

3.3.1 VGG-16 Model

The VGG-16 [39] was trained on an extensive dataset containing more than a million images sourced from ImageNet. It comprises a total of 19 layers and possesses the capability to categorize images into 1000 distinct classes, including a wide range of categories including animals, as well as everyday objects such as computers, chairs, and pencils. The network has acquired the ability to generate diverse and comprehensive feature representations that are well-suited for effective skin cancer dermoschopic image classification. For image analysis using this network, the input skin cancer image must follow to a fixed shape of [224, 224, 3], equivalent to 224x224 pixels, with the number 3 indicating the presence of RGB channels. The only required preprocessing step involves subtracting the mean RGB value from each pixel throughout the entire training dataset.

During the 2014 ILSVR (ImageNet) competition, VGG16, a CNN architecture featured in the illustration, secured victory. This design has gained acclaim as one of the most exceptional vision model architectures ever devised. VGG16 stands out for its focus on 3x3 filter convolution layers with a stride of 1, as well as its consistent utilization of 2x2 filter stride 2 for max pooling and padding layers. The architecture maintains an even distribution of convolution and max pool layers [40]. Finally, seven dense layers with SoftMax as the activation function are introduced. VGG16 consists of 16 layers with varying weights. This model, in integrated with VGG-19 and ResNet-50, to accurately classify the type of skin cancer.

- A reduced network size.
- High computing speed.
- This model applies incremental learning for improved classification ability, fast computation, and decrease deprivation.

3.3.2 VGG-19 Model

This model is the extension of VGG-16 and introduced in 2014 by Simonyan and colleagues [44]. The architecture of this model is based on Convolutional networks (ConvNet). It consists of 19 layers which are organized stacks convolutional layer, pooling layer, and fully connected/dense layer. In this research work, this model is utilized as feature extractor from skin cancer image dataset. This pre-trained model is fine-tuned. Seven fully connected layers are added for our dataset on the top of this model.

3.3.3 ResNet-50 Model

Due to the skin cancer dataset's significantly limited number of labeled images in comparison to the ten million labeled images found in ImageNet, the training of deep CNN models for skin cancer classification becomes a challenging task, resulting in reduced accuracy in model estimations. Nevertheless, implementing the capabilities of transfer learning allows us to achieve robust performance with deep CNN models that were originally trained on ImageNet, even when opposed with small datasets in diverse domains, such as automated medical image analysis, including the detection of skin cancer from dermoscopic images. In this research, we actively employ the ResNet-50 model [39], pre-trained on ImageNet, for the purpose of skin cancer classification. As its depth increases, ResNet-50 rapidly achieves

higher accuracy. Due to ResNet-50's outstanding classification capabilities and its ability to extract robust features from images, we hypothesize that the feature extraction layers within ResNet-50 will excel when applied to medical image classification. A pivotal component of ResNet-50 is the use of residual blocks (RB) as shown in figure 4. RB relies on the concept of employing shortcut connections to bypass specific convolutional layers. These techniques play a critical role in enhancing training parameters during error backpropagation, effectively tackling the challenge of vanishing gradients. Therefore, this facilitates the development of deeper CNN structures, ultimately resulting in improved performance in skin cancer classification. These residual blocks are composed of multiple convolutional layers (Conv), batch normalizations, ReLU activation functions (BN), and a single shortcut. Suppose f is non-linear function in RB for convolutional path, then output is computed as follows:

$$y = f(x) + x \tag{2}$$

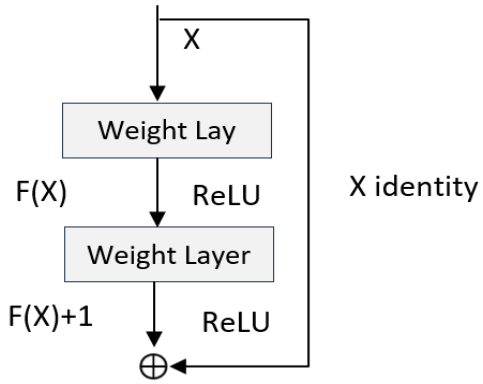

Figure 4. Residual block (RB): A building block of ResNet-50 representing X as input and then processed by ReLU [39].

Several RB blocks are applied in this model as published in [39] and applied in this research work for extracting features from skin cancer dataset. All of these models (ResNet-50, VGG-16, and VGG-19) are applied to extract features from skin cancer dataset. These features are then combined to generate a composite feature vector.

3.3.4 Layers for feature extraction

The MMF-SCD model consists of various layers namely: input layer, convolutional layer, activation layer, max-pooling layer, flatten and dense layers. A stack of these layers is utilized to build the model. These layers are defined in the table 4 and 5 as follows:

Table 4. Layered architecture of VGG-16 representing stack of neural network layers is sequence**.**

VGG-16 Layers	**Input/output**	**Shape of input/out-put**
Convolution	Input	(None,224x224x3)
Convolution2D	Output	(None,224x224x64)
Convolution	Input	(None,224x224x64)
Convolution2D	Output	(None,224x224x64)
pooling	Input	(None,224x224x64)
Maxpoolinging2D	Output	(None,112x112x64)
Convolution	Input	(None,112x112x64)
Convolution2D	Output	(None,112x112x128)

Convolution	Input	(None,112x112x128)
Convolution2D	Output	(None,112x112x128)
pooling	Input	(None,112x112x128)
Maxpoolinging2D	Output	(None,56x56x128)
Convolution	Input	(None,56x56x128)
Convolution2D	Output	(None,56x56x256)
Convolution	Input	(None,56x56x256)
Convolution2D	Output	(None,56x56x256)
Convolution	Input	(None,56x56x256)
Convolution2D	Output	(None,56x56x256)
pooling	Input	(None,56x56x256)
Maxpoolinging2D	Output	(None,28x28x256)
Convolution	Input	(None,28x28x256)
Convolution2D	Output	(None,28x28x512)
Convolution	Input	(None,28x28x512)
Convolution2D	Output	(None,28x28x512)
Convolution	Input	(None,28x28x512)
Convolution2D	Output	(None,28x28x512)
pooling	Input	(None,28x28x512)
Maxpoolinging2D	Output	(None,14x14x512)
Convolution	Input	(None,14x14x512)
Convolution2D	Output	(None,14x14x512)
Convolution	Input	(None,14x14x512)
Convolution2D	Output	(None,14x14x512)
Convolution	Input	(None,14x14x512)
Convolution2D	Output	(None,14x14x512)
pooling	Input	(None,14x14x512)
Maxpoolinging2D	Output	(None,7x7x512)
flatten 1	Input	(None,7x7x512)
Flatten	Output	(None,25088)
Dense 2	Input	(None,25088)
Dense	Output	(None,7)

Table 5. Layered architecture of VGG-19 representing stack of neural network layers is sequence**.**

VGG-19 Layers	Input/Output	Shape of input/output
Convolution	Input	(None,224,224,3)
Convolution2D	Output	(None,224x224x64)
Convolution	Input	(None,224x224x64)
Convolution2D	Output	(None,224x224x64)
pool	Input	(None,224x224x64)
MaxPooling2D	Output	(None,112x112x64)
Convolution	Input	(None,112x112x64)
Convolution2D	Output	(None,112x112x128)
Convolution	Input	(None,112x112x128)
Convolution2D	Output	(None,112x112x128)

pool	Input	(None,112x112x128)
MaxPooling2D	Output	(None,56x56x128)
Convolution	Input	(None,56x56x128)
Convolution2D	Output	(None,56x56x256)
Convolution	Input	(None,56x56x256)
Convolution2D	Output	(None,56x56x256)
Convolution	Input	(None,56x56x256)
Convolution2D	Output	(None,56x56x256)
Convolution	Input	(None,56x56x256)
Convolution2D	Output	(None,56x56x256)
pool	Input	(None,56x56x256)
MaxPooling2D	Output	(None,28x28x256)
Convolution	Input	(None,28x28x256)
Convolution2D	Output	(None,28x28x512)
Convolution	Input	(None,28x28x512)
Convolution2D	Output	(None,28x28x512)
Convolution	Input	(None,28x28x512)
Convolution2D	Output	(None,28x28x512)
Convolution	Input	(None,28x28x512)
Convolution2D	Output	(None,28x28x512)
pool	Input	(None,28x28x512)
MaxPooling2D	Output	(None,14x14x512)
Convolution	Input	(None,14x14x512)
Convolution2D	Output	(None,14x14x512)
Convolution	Input	(None,14x14x512)
Convolution2D	Output	(None,14x14x512)
Convolution	Input	(None,14x14x512)
Convolution2D	Output	(None,14x14x512)
Convolution	Input	(None,14x14x512)
Convolution2D	Output	(None,14x14x512)
pool	Input	(None,14x14x512)
MaxPooling2D	Output	(None,7x7x512)
flatten	Input	(None,7x7x512)
Flatten	Output	(None,25088)
dense	Input	(None,25088)
Dense	Output	(None,7)

3.3.5 Input layer

The first layer which receives pre-processed (resized and rescaled) skin cancer images is input layer. This layer has tensors of skin cancer images with 224x224 dimensions of pixel values. This layer transfers all these images to convolutional layer.

3.3.6 Convolutional layer

This layer is responsible for extracting features [41] from skin-cancer images based on number of filters defined as a parameters, and it plays a vital role, as a building block in CNN. This layer is designed on a mathematical function called convolution operation which extracts features (i.e., shape, color, edges) from input images. This layer preserves all the parameters and weights learned during the training phase. The

tensors within these layers exhibit lower values compared to the input layer but possess greater depth. Furthermore, this layer stores both training configurations and weight information as follows:

$$M_P = \left(k_1 * k_2 * M_{input} * M_{output} + M_{bias}\right) \quad (3)$$

$k_1$and k_2 are kernals, M_{input} and M_{output} are number of input and output filters respectively. Where,

$$M_{output} = M_{bias} \quad (4)$$

Feature maps are generated as a results of convolution operations.

In this network, the convolutional layer employs a 3x3 kernel size with a one-pixel stride, ensuring coverage across the entire image. Spatial padding is incorporated to maintain the image's spatial resolution. Additionally, maximum pooling is executed using a 2x2 pixel window and a stride of 2. Notably, N signifies the input image's size, s represents the stride value, and f corresponds to the filter size then convolution is computed as follows:

N=224, s=1, f=3x3, size of padding (ps)=1, 64 is the number of applied filters,

$$Conv_1 = \left[\frac{N-f}{ps}\right] + 1 = \left[\frac{224-3}{1}\right] + 1 = 222 \quad (5)$$

The feature map (f_{map}) is computed as:

$$f_{map} = \left[\frac{224-3+2}{1}\right] + 1 = 224 \quad (6)$$

This has output channel of shape $[224x224x64]$.

Now, N=222, ps=1, and f=3

$$Conv_2 = \left[\frac{N-f}{ps}\right] + 1 = \left[\frac{222-3}{1}\right] + 1 = 220 \quad (7)$$

This has output channel of shape $[220x220x64]$.

For third convolutional layer ($Conv_3$), N=220, ps=1, and f=3

$$Conv_3 = \left[\frac{N-f}{ps}\right] + 1 = \left[\frac{220-3}{1}\right] + 1 = 218 \quad (8)$$

For $Conv_4$ N=218, ps=1, and f=3

$$Conv_4 = \left[\frac{N-f}{ps}\right] + 1 = \left[\frac{218-3}{1}\right] + 1 = 216 \quad (9)$$

For $Conv_5$ N = 216, ps=1, and f=3

$$Conv_5 = \left[\frac{N-f}{ps}\right] + 1 = \left[\frac{216-3}{1}\right] + 1 = 214 \quad (10)$$

Similarly, the thirteenth convolutional layer $Conv_{13}$ produced the following:

$$Conv_{13} = \left[\frac{N-f}{ps}\right] + 1 = \left[\frac{16-3}{1}\right] + 1 = 14 \quad (11)$$

Each feature detector in the convolutional layer recognizes and extracts crucial elements from the input skin cancer image, producing a feature map that assists in predicting their future spatial distribution. The architecture of CNN based algorithms is based on neurons arranged and connected in specific way and compute according to human brain simulations. In simple words a neuron is a node in neural network through which data flows and computations are passed. Suppose *m*x*m* is the size of neuron layer, *n*x*n* is the filter *w*, then output of layer will have size of:

$$output = (m-n+1)\text{x}(m-n+1) \quad (12)$$

Contributions of each layer is summed to compute non-linearity in one unit X_{ij}^l:

$$X_{ij}^l = \sum_{a=0}^{n-1}\sum_{b=0}^{n-1} w_{ab} y_{(i+a)(j+b)}^{l-1} \quad (13)$$

The non-linearity of this convolution function is computed as follows:

$$y_{ij}^{l} = \sigma(X_{ij}^{l}) \quad (14)$$

3.3.7 Activation function

Like a conventional artificial neural network, the feature maps undergo processing by an activation function. Specifically, they pass through a rectifier function, which yields a value of 0 for inputs below 0 and retains the input value otherwise [42]. The working principle is computed in equation and shown in Figure 6.

$$ReLU = max(0,a) = \begin{cases} a \; if \; a > 0 \\ 0 \; if \; a \leq 0 \end{cases} \quad (15)$$

Here, a is the input and max() is function of ReLU.

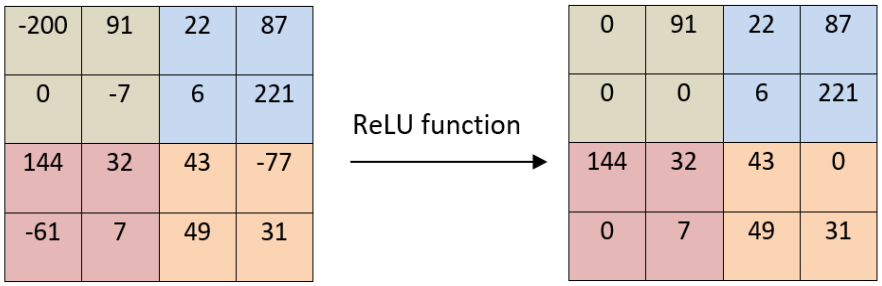

Figure 5. Working principle demonstration of ReLU function, 4x4 table at left is input and table at right is output by ReLU function.

To infuse non-linearity into the model, ReLU is employed, resulting in reduced computation time and improved classification performance. Unlike previous studies that relied on tanh and sigmoid functions, ReLU has proven greater. Its computational efficiency and lack of saturation contribute to this dominance.

3.3.8 Pooling layer

This layer, as implied by its name, utilizes incoming tensors from subsequent layers to identify the most favorable features. The dimension of the resulting tensor depends on the size of the kernel in the input tensors [41]. For instance, if the kernel size is eight, the final result is divided by eight. Following the completion of feature extraction and pooling operations, the composite model incorporates seven fully connected layers. The initial two layers possess 4096 dimensions each, while the seventh layer consists of seven channels. These layers utilize the feature maps generated by the convolutional layers to generate the ultimate classification outcome. In the case where the input size N equals 112, the filter size f is 2, the stride is 2, and no padding is applied, the subsequent formula is employed for max pooling calculation:

$$Pooling_{max} = [\ \frac{112-2+0}{2}]+ \quad 1 = \quad 56 \quad (16)$$

$$Output = \ 56 \ x \ 56 \ x \ 128 \quad (17)$$

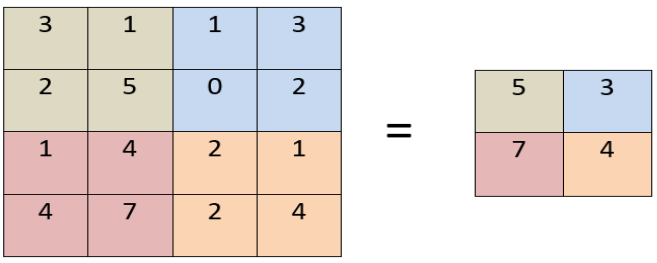

Figure 6. Working principle demonstration of pooling layer, 4x4 feature matrix is input and 2x2 is output after pooling.

3.4 Feature Optimization

The above applied layers (convolutional layer, pooling layer) perform feature extraction, and then these extracted features are combined. Concatenate () function is applied to combine all features together extracted from VGG-16, VGG-19, and ResNet-50. These features are optimized using Adam [43]. It is a popular optimizer which has gained success in deep learning for image classification and identification. During training, an algorithm known as an optimizer is employed to minimize model loss through adjustments to the network weights. Convolutional neural networks can be optimized using a variety of optimizers, including Adam, AdaGrad, RMSProp, stochastic gradient descent (SGD) and others.

3.5 Training and evaluation of proposed model

This study work employs a transfer learning approach to develop the MMF-SCD. This approach enhances performance, reduces development time, minimizes computing resource requirements, and results in a model with superior classification potential. It utilizes pre-trained weights and structure for a skin cancer dataset.

The proposed MMF-SCD model is trained on ISIC skin cancer dataset and validated on validation dataset. The MMF-SCD uses this dataset (training portion), which has examples from all image categories and is the biggest part of the data. Image classifiers use image datasets to teach and evaluate themselves. These datasets have collections of sample images from the real world. MMF-SCD is supervised model and trained with an image dataset that has labels, and these labeled images are the basis for the MMF-SCD to learn. Training data, which is the information used to teach the CNN algorithm or any image-classification model (i.e., MMF-SCD), is important in the classification process. Training data helps the model get better at recognizing. Model training is a way to teach a MMF-SCD model how detects cancer diseases. At first, neural networks look at a lot of labeled data, and this helps them get better at handling new data later on, using what they've learned before. In the MMF-SCD training process, the validation dataset checks how well the model works and prevents it from learning too much.

Various evaluation metrics are applied to evaluate the performance of MMF-SCD for skin cancer identification using dermoscopic images as input file. Accuracy, loss, recall, f1-score, and precision are advance evaluation metrics employed in this research work. To measure these metrics, four basic parameters are calculated after training and validation that are true positive prediction (TPP), true negative prediction (TNP), false positive prediction (FPP), and false negative (FNP). These parameters are calculated as follows:

TPP: Correct positive predictions by MMF-SCD for skin cancer classification.

TNP: Correct negative predictions by MMF-SCD for skin cancer classification.

FPP: Incorrect positive predictions by MMF-SCD for skin cancer classification.

FNP: Incorrect negative predictions by MMF-SCD for skin cancer classification.

3.5.1 Accuracy

Accuracy is an important evaluation parameter for checking the performance of machine learning and deep learning models. The accuracy ranges between 0%-100%, where 100% represents highest accuracy with better classification ability of model. It is calculated by following mathematical equation:

$$Accuracy = \frac{TPP+TNP}{TPP+TNP+FPN+FNN} \quad (18)$$

3.5.2 Precision

When evaluating deep learning models, it is crucial to emphasize precision as a fundamental aspect. In the symphony of algorithms, precision emerges as the virtuoso, crafting melodies of accuracy that

resonate through the digital realm. Imagine it as a keen-eyed detective, discerning the true gems from a trove of images. With a mathematician's grace, it calculates the purity of its predictions, creating harmony between the algorithm's prowess and the dataset's nuances. Precision, the maestro of relevance, conducts a symphony where every note resonates with the essence of truth. It is calculated by following mathematical equation:

$$Precision = \frac{TPP}{TPP+FPP} \tag{19}$$

3.5.3 Recall

Recall is also an important evaluation metrics for checking MMF-SCD model performance for skin cancer disease classification. It calculates the proportion of accurately identified relevant skin cancer images. A model achieves perfect recall when it correctly identifies all relevant images with a score exceeding a specific threshold; otherwise, it represents lower recall. The total count of relevant skin cancer images serves as a benchmark for evaluating the model's effectiveness in classification of these images.
It is calculated by following mathematical equation:

$$Recall = \frac{TPP}{TPP+FNP} \tag{20}$$

3.5.4 F1 Score

This parameter is referred as more effective than accuracy of model. The F1 score serves as a metric employed in assessing deep learning models (i.e., in our study MMF-SCD model), including applications in skin cancer classification. It combines precision and recall, present a unified assessment of a model's effectiveness. It is calculated by following mathematical equation:

$$F1\ score = 2 * \frac{Recall*Precision}{Recall+Precision} \tag{21}$$

3.6 Model Predictions

The final layers in the MMF-SCD are *"fully connected"* which are responsible for classification and predictions using the SoftMax activation function [44]. Within this layer, training outcomes and weights are stored, enabling the identification of the most probable classes for computing classification probabilities. When the kernel size is one, it can establish the following parameters.

$$M_{Param} = \left(M_{input} * M_{output} + M_{bias}\right) \tag{22}$$

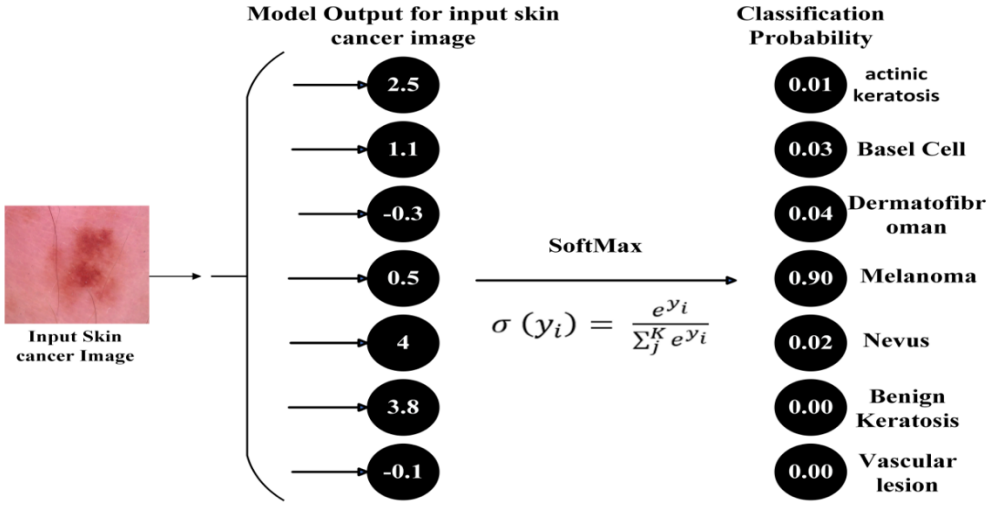

Figure 7. SoftMax activation results demonstration for model prediction probability counting.

In its capacity as the last functional layer in the network, the SoftMax function calculates the probability of each input skin cancer image being associated with specific classes related to skin cancer diseases as shown in Figure 9. It transforms the output from the previous layer into a probability distribution encompassing the seven categories on which the composite network was trained. This enables the network to make predictions about the input image by choosing the category with the highest probability, ensuring that the total probabilities across all categories sum to one. If y_i denotes the ith input vector, and σ represents the SoftMax function [44], the output is computed as follows:

$$\sigma\,(y_i) = \frac{e^{y_i}}{\sum_j^K e^{y_i}} \tag{23}$$

Here, e^{y_i} is exponential function of input vector, exponential function of output vector (j), and number of classes are presented by K which is seven in this study work. The visual demonstration of classification using softmax activation function is presented in Figure 9.

3.7 Experiment environment

In this study, a computing platform based on a Google Collaborator Python notebook was employed to facilitate live coding and outcome analysis. This cloud-based technology enhances the ease of sharing and replicating scientific research, allowing access to tests and findings even offline.

4. Results

The proposed MMF-SCD model resulted in comparatively high accuracy rate of 97.6%. These results are shown in figure:

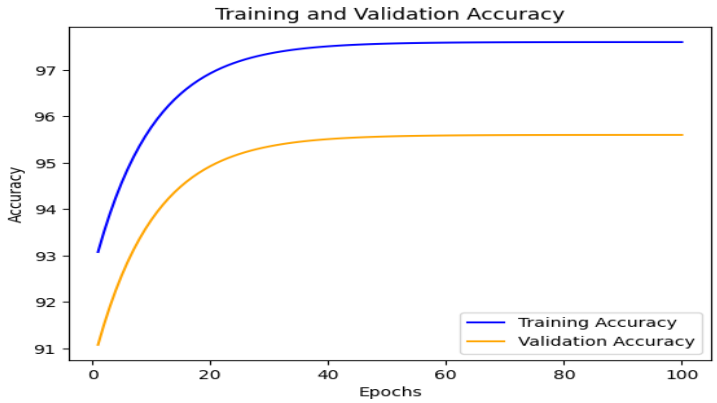

Figure 8. Line graph of model accuracy. The blue line indicates training accuracy and orange line represents validation accuracy.

Whereas, the following Figure 11 represents model loss in form of line graph.

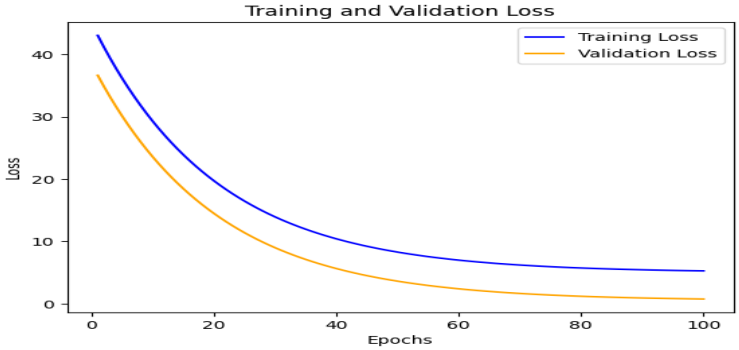

Figure 9. Line graph of model loss. Blue line indicates training loss of model whereas orange line represents validation loss.

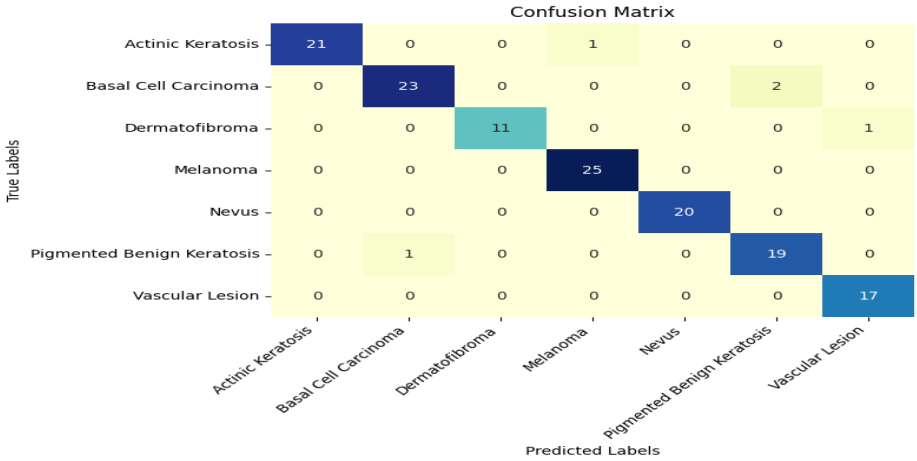

Figure 10. Confusion matrix of model predictions, in the diagonal of this matrix all the numbers represent accurately classified number of images by MMF-SCD, whereas only five images are misclassified.

The results of MMF-SCD are also represented in the form of confusion matrix, where confusion matrix is a table which demonstrates model performance in the form of predicted values and actual values. The X-axis represents predicted labels and Y-axis represents actual labels. The following bar graph (Figure 13) represents precision, recall, and f1-score values as a result of model predictions.

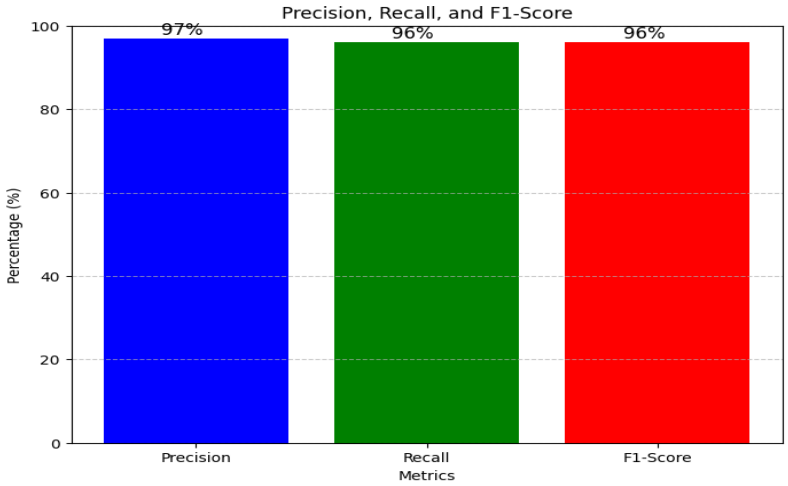

Figure 11. Bar graph of evaluation matrices representing precision, recall, and f1-score

The blue bar represents precision, green one represents recall metrics while red shows F1-score. The precision of model prediction is 97% whereas, the recall and F1-score has 96%.

The following table 6 and bar graph figure 14 represents benchmark comparison of proposed methodology.

Table 6. Comparison of benchmark works with proposed MMF-SCD

Ref No.	Diagnosis	Dataset	Technique	Accuracy Results
[26]	Melanoma, Melanocytic nevus, Basal cell carcinoma, Actinic keratosis, Benign keratosis-like lesions,	HAM10000 dataset (Consists of 10,015 dermatoscopy images)	Xception, Densenet, Mobilenet, Resnet-50, VGG-16, Inceptionv3, CNN	90%

	Dermatofibroma, Vascular lesions			
[27]	basal cell carcinoma, melanoma, squamous cell carcinoma, and Nevus	ISIC 2020, DermIS, HAM10000	DSCC_Net, deep learning	94.17%
[28]	basal cell carcinoma, melanoma, squamous cell carcinoma, and Nevus	HAM10000 dataset	deep learning, Android app, fine tuning of CNN, Explainable Artificial Intelligence	82%
[30]	Seven categories: basal cell carcinoma, melanoma, squamous cell carcinoma, and Nevus	HM10000	automated classification, CNN,	92.90%
[31]	basal cell carcinoma, melanoma, squamous cell carcinoma, and Nevus	HAM10000	MobileNet, VGG-16, VGG-19, and InceptionV3	89.81%.
[34]	basal cell carcinoma, melanoma, squamous cell carcinoma, and Nevus	HAM10000	Xception model, augmentation of images	96%
Proposed	**actinic keratosis, basal cell carcinoma, dermatofibroma, melanoma, nevus, pigmented benign**	**ISIC**	**MMF-SCD**	**97.6%**

	keratosis, and vascular lesion

The above table shows the benchmark comparison of work of other authors related to skin cancer.

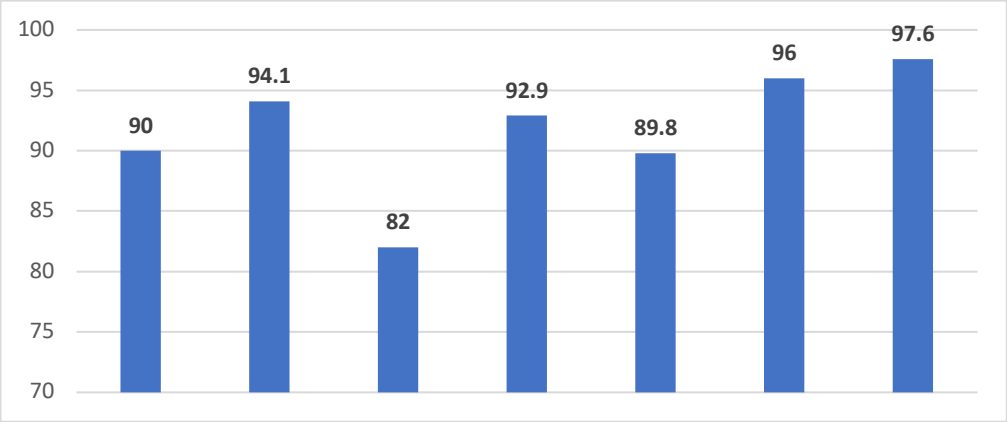

Figure 12. Bar graph of benchmark comparison of proposed MMF-SCD with results of recent studies in the literature work.

It is evident from the above table and bar graph that our model MMF-SCD has the highest accuracy (97.6%) among the earlier developed models used to classify various types of skin cancers.

5. Conclusion

Skin cancer affects a considerable number of people on a daily basis and is a major contributor to related fatalities. Consequently, the identification and classification of various skin cancer types are crucial for early screening and treatment. Current clinical diagnostic procedures are vulnerable to human errors, often due to the inexperience of physicians and native subjectivity. During the last decades, deep learning has shown remarkable success in medical field including skin cancer identification and classification. This thesis introduced an efficient method for reducing the number of false diagnoses and eliminating subjectivity in the visual interpretation of dermoscopic images for skin cancer classification. It is achieved by presenting a composite feature extraction approach and introducing the Multi-Model Fusion for Skin Cancer Detection (MMF-SCD). The ISIC skin cancer dataset utilized is publically available at Kaggle website. It has seven classes namely: actinic keratosis, basal cell carcinoma, dermatofibroma, melanoma, nevus, pigmented benign keratosis, and vascular lesion.

Data augmentation is applied using image data generator by TensorFlow to generate augmented images at real time during trainig process of MMF-SCD for better model development. Transfer learning approach is adopted to train the model with reduced computatational cost and time. The applied MMF-SCD model is evaluetd in terms of various evaluation metrices namely: accuracy of model (97.6%), loss of model (5%), f1-score (96%), precision (97%), and recall (96%). These results demonstrate that model has gained high accuracy for the identification and classification of skin cacner. The suggested approach could be applied for cancer classification in real time applications to assist specialists and novice physicians in diagnosis at health care centers.

6. Future Work

The presented research work could be expanded to some other image based modalities with high precision and accuracy rates for medical image analysis and disease identification such as lungs cancer detection, brain tumor identification, and classification of eye diseases. Therefore, in this domain proposed MMF-SCD model is suitable for appliactions having similar issues.

References

1. "WHO: Global health observatory data repository - Google Scholar." Accessed: Sep. 10, 2023. [Online].
2. H. S. Han and K. Y. Choi, "Advances in Nanomaterial-Mediated Photothermal Cancer Therapies: Toward Clinical Applications," Biomedicines 2021, Vol. 9, Page 305, vol. 9, no. 3, p. 305, Mar. 2021, doi: 10.3390/BIOMEDICINES9030305.
3. D. Hee Lee and S. N. Yoon, "Application of Artificial Intelligence-Based Technologies in the Healthcare Industry: Opportunities and Challenges," International Journal of Environmental Research and Public Health 2021, Vol. 18, Page 271, vol. 18, no. 1, p. 271, Jan. 2021, doi: 10.3390/IJERPH18010271.
4. G. Di Leo, C. Liguori, A. Paolillo, and P. Sommella, "A web-based application for dermoscopic measurements and learning," in 2015 IEEE International Symposium on Medical Measurements and Applications (MeMeA) Proceedings, IEEE, 2015, pp. 279–284.
5. A. Naeem, T. Anees, M. Fiza, R. A. Naqvi, and S.-W. Lee, "SCDNet: A Deep Learning-Based Framework for the Multiclassification of Skin Cancer Using Dermoscopy Images," Sensors, vol. 22, no. 15, p. 5652, 2022.
6. A. Naeem, M. S. Farooq, A. Khelifi, and A. Abid, "Malignant melanoma classification using deep learning: datasets, performance measurements, challenges and opportunities," IEEE access, vol. 8, pp. 110575–110597, 2020.
7. K. M. Hosny and M. A. Kassem, "Refined residual deep convolutional network for skin lesion classification," J Digit Imaging, vol. 35, no. 2, pp. 258–280, 2022.
8. Y. Nie, L. De Santis, M. Carratù, M. O'Nils, P. Sommella, and J. Lundgren, "Deep melanoma classification with K-fold cross-validation for process optimization," in 2020 IEEE international symposium on medical measurements and applications (MeMeA), IEEE, 2020, pp. 1–6.
9. Y. Nie, P. Sommella, M. O'Nils, C. Liguori, and J. Lundgren, "Automatic detection of melanoma with yolo deep convolutional neural networks," in 2019 E-Health and Bioengineering Conference (EHB), IEEE, 2019, pp. 1–4.
10. S. Riaz, A. Naeem, H. Malik, R. A. Naqvi, and W.-K. Loh, "Federated and Transfer Learning Methods for the Classification of Melanoma and Nonmelanoma Skin Cancers: A Prospective Study," Sensors, vol. 23, no. 20, p. 8457, 2023.
11. R. Sinclair, C. Baker, L. Spelman, M. Supranowicz, and B. MacMahon, "A review of actinic keratosis, skin field cancerisation and the efficacy of topical therapies," Australasian Journal of Dermatology, vol. 62, no. 2, pp. 119–123, 2021.
12. L. Hogue and V. M. Harvey, "Basal cell carcinoma, squamous cell carcinoma, and cutaneous melanoma in skin of color patients," Dermatol Clin, vol. 37, no. 4, pp. 519–526, 2019.
13. Y. N. Fu'adah, N. K. C. Pratiwi, M. A. Pramudito, and N. Ibrahim, "Convolutional neural network (cnn) for automatic skin cancer classification system," in IOP conference series: materials science and engineering, IOP Publishing, 2020, p. 012005.
14. O. Sevli, "A deep convolutional neural network-based pigmented skin lesion classification application and experts evaluation," Neural Comput Appl, vol. 33, no. 18, pp. 12039–12050, 2021.
15. N. Gouda and J. Amudha, "Skin cancer classification using ResNet," in 2020 IEEE 5th International Conference on Computing Communication and Automation (ICCCA), IEEE, 2020, pp. 536–541.
16. E. Vocaturo, D. Perna, and E. Zumpano, "Machine learning techniques for automated melanoma detection," in 2019 IEEE International Conference on Bioinformatics and Biomedicine (BIBM), IEEE, 2019, pp. 2310–2317.
17. A. Javaid, M. Sadiq, and F. Akram, "Skin cancer classification using image processing and machine learning," in 2021 international Bhurban conference on applied sciences and technologies (IBCAST), IEEE, 2021, pp. 439–444.
18. S. Jinnai, N. Yamazaki, Y. Hirano, Y. Sugawara, Y. Ohe, and R. Hamamoto, "The development of a skin cancer classification system for pigmented skin lesions using deep learning," Biomolecules, vol. 10, no. 8, p. 1123, 2020.
19. I. Kousis, I. Perikos, I. Hatzilygeroudis, and M. Virvou, "Deep learning methods for accurate skin cancer recognition and mobile application," Electronics (Basel), vol. 11, no. 9, p. 1294, 2022.
20. M. Dildar et al., "Skin cancer detection: a review using deep learning techniques," Int J Environ Res Public Health, vol. 18, no. 10, p. 5479, 2021.

21. A. Mahbod, G. Schaefer, C. Wang, R. Ecker, and I. Ellinge, "Skin lesion classification using hybrid deep neural networks," in ICASSP 2019-2019 IEEE International Conference on Acoustics, Speech and Signal Processing (ICASSP), IEEE, 2019, pp. 1229–1233.
22. D. B. Mendes and N. C. da Silva, "Skin lesions classification using convolutional neural networks in clinical images," arXiv preprint arXiv:1812.02316, 2018.
23. M. Q. Hatem, "Skin lesion classification system using a K-nearest neighbor algorithm," Vis Comput Ind Biomed Art, vol. 5, no. 1, pp. 1–10, 2022.
24. A. Murugan, S. A. H. Nair, and K. P. S. Kumar, "Detection of skin cancer using SVM, random forest and kNN classifiers," J Med Syst, vol. 43, pp. 1–9, 2019.
25. A. Atta, M. A. Khan, M. Asif, G. F. Issa, R. A. Said, and T. Faiz, "Classification of Skin Cancer empowered with convolutional neural network," in 2022 International Conference on Cyber Resilience (ICCR), IEEE, 2022, pp. 1–6.
26. M. S. Akter, H. Shahriar, S. Sneha, and A. Cuzzocrea, "Multi-class skin cancer classification architecture based on deep convolutional neural network," in 2022 IEEE International Conference on Big Data (Big Data), IEEE, 2022, pp. 5404–5413.
27. M. Tahir, A. Naeem, H. Malik, J. Tanveer, R. A. Naqvi, and S.-W. Lee, "DSCC_Net: Multi-Classification Deep Learning Models for Diagnosing of Skin Cancer Using Dermoscopic Images," Cancers (Basel), vol. 15, no. 7, p. 2179, 2023.
28. K. Mridha, M. M. Uddin, J. Shin, S. Khadka, and M. F. Mridha, "An Interpretable Skin Cancer Classification Using Optimized Convolutional Neural Network for a Smart Healthcare System," IEEE Access, 2023.
29. L. I. Mampitiya, N. Rathnayake, and S. De Silva, "Efficient and low-cost skin cancer detection system implementation with a comparative study between traditional and CNN-based models," Journal of Computational and Cognitive Engineering, vol. 2, no. 3, pp. 226–235, 2023.
30. K. Polat and K. O. Koc, "Detection of skin diseases from dermoscopy image using the combination of convolutional neural network and one-versus-all," Journal of Artificial Intelligence and Systems, vol. 2, no. 1, pp. 80–97, 2020.
31. M. A. Ratul, M. H. Mozaffari, W. S. Lee, and E. Parimbelli, "Skin lesions classification using deep learning based on dilated convolution, bioRxiv, 860700." 2019.
32. J. Rashid et al., "Skin cancer disease detection using transfer learning technique," Applied Sciences, vol. 12, no. 11, p. 5714, 2022.
33. M. S. Ali, M. S. Miah, J. Haque, M. M. Rahman, and M. K. Islam, "An enhanced technique of skin cancer classification using deep convolutional neural network with transfer learning models," Machine Learning with Applications, vol. 5, p. 100036, 2021.
34. L. Moataz, G. I. Salama, and M. H. Abd Elazeem, "Skin cancer diseases classification using deep convolutional neural network with transfer learning model," in Journal of physics: conference series, IOP Publishing, 2021, p. 012013.
35. T. Saba, M. A. Khan, A. Rehman, and S. L. Marie-Sainte, "Region extraction and classification of skin cancer: A heterogeneous framework of deep CNN features fusion and reduction," J Med Syst, vol. 43, no. 9, p. 289, 2019.
36. U.-O. Dorj, K.-K. Lee, J.-Y. Choi, and M. Lee, "The skin cancer classification using deep convolutional neural network," Multimed Tools Appl, vol. 77, pp. 9909–9924, 2018.
37. "Skin Cancer | Kaggle." Accessed: Sep. 20, 2023. [Online]. Available: https://www.kaggle.com/datasets/gabrielmv/skin-cancer
38. A. Yang, X. Yang, W. Wu, H. Liu, and Y. Zhuansun, "Research on feature extraction of tumor image based on convolutional neural network," IEEE access, vol. 7, pp. 24204–24213, 2019.
39. K. Simonyan and A. Zisserman, "Very deep convolutional networks for large-scale image recognition," arXiv preprint arXiv:1409.1556, 2014.
40. S. Mascarenhas and M. Agarwal, "A comparison between VGG16, VGG19 and ResNet50 architecture frameworks for Image Classification," Proceedings of IEEE International Conference on Disruptive Technologies for Multi-Disciplinary Research and Applications, CENTCON 2021, pp. 96–99, 2021, doi: 10.1109/CENTCON52345.2021.9687944.
41. L. Liu, C. Shen, and A. Van den Hengel, "The treasure beneath convolutional layers: Cross-convolutional-layer pooling for image classification," in Proceedings of the IEEE conference on computer vision and pattern recognition, 2015, pp. 4749–4757.
42. A. F. Agarap, "Deep learning using rectified linear units (relu)," arXiv preprint arXiv:1803.08375, 2018.

43. D. P. Kingma and J. L. Ba, "Adam: A Method for Stochastic Optimization," 3rd International Conference on Learning Representations, ICLR 2015 - Conference Track Proceedings, Dec. 2014, Accessed: May 04, 2023. [Online]. Available: https://arxiv.org/abs/1412.6980v9
44. "Understanding Categorical Cross-Entropy Loss, Binary Cross-Entropy Loss, Softmax Loss, Logistic Loss, Focal Loss and all those confusing names." Accessed: Mar. 18, 2023. [Online]. Available: https://gombru.github.io/2018/05/23/cross_entropy_loss/